Available online at www.sciencedirect.com

ScienceDirect

Materials Today: Proceedings 13 (2019) 181–186

materialstoday: PROCEEDINGS

www.materialstoday.com/proceedings

ICAMST 2018

The Effect of Reduced Graphene Oxide on the Activated Carbon Metal Oxide Supercapacitor

Harsojo[a,*], Maryati Doloksaribu[a], Bambang Prihandoko[b], Slamet Priyono[b], Achmad Subhan[b], Titik Lestariningsih[b]

[a]*Departemen of Physics, University Gadjah Mada, Yogyakarta, Indonesia*
[b]*Pusat Penelitian Fisika, LIPI Serpong, Indonesia*

Abstract

We studied the effect of reduced graphene oxide (RGO) materials on the supercapacitors made of activated carbon and transition metal oxides (ACMO). We tested the supercapacitors using two-probe cyclic voltammetry (CV) and checked the impedance using electrochemical impedance spectroscopy (EIS) at a frequency up to MHz. The results indicated that the 5% of the metal oxide in the ACMO increased the surface area and the capacitance. However, the addition of a low concentration of RGO (2%) to the ACMO decreased it.

Peer-review under responsibility of the scientific committee of The 6th International Conference on Advanced Materials Science and Technology 2018, 6th ICAMST.

Keywords: supercapacitor; graphene oxide; CuO; MnO_2; TiO_2

1. Introduction

Many authors had investigated supercapacitors based on activated carbon (AC) materials [1-5]. The reason is that the AC has a high surface area (in the order of 1000 m^2g^{-1}) and macroporous and mesoporous phases. These quantities are suites for energy storage based on the electric double layer (EDLC) mechanism in which the depletion of the oppositely charged species stores the energy at the interface of the electrode and the electrolyte. The specific

* Corresponding author. Tel.: +62-821-3753-3438; fax: +62-274545185.
E-mail address: harsojougm@ugm.ac.id

Peer-review under responsibility of the scientific committee of The 6th International Conference on Advanced Materials Science and Technology 2018, 6th ICAMST.

capacitance of EDLC measured as $C = \varepsilon A/d$, where ε is the dielectric of materials, A is the surface area, d is the distance between the opposite charge. This EDLC mechanism generates a high charge-discharge rate. The energy of the supercapacitor is $E = CV^2/2$, and the power is $P = V^2/R_s$, where V is the window voltage, R_s is the total series resistance. However, the activated carbon supercapacitor (ACS) has some drawbacks because it has a limited capacitance (about 150 Fg^{-1}). Using aqua based electrolyte, the maximum potential windows to store the energy in ACS is about 1 volt making it a smaller energy density compared to the battery.

Meanwhile, the resistance of ACS is high, since AC is not a good conductor. Therefore, to improve the performance it requires other than EDLC mechanism in storing the energy. This mechanism is commonly known to the pseudo supercapacitor (PSC). In contrast to EDLC, in the PSC energy is stored by faradaic process or redox process. In such a storing, the capacitance measured as $C = nF/MV$, where n is the number of electrons, F Faraday number, M molar, and V window voltage. Since such a process happens on the interface of materials and the electrolyte, therefore, the nanostructure metal oxide (MO) will be able to serve it. The simple form of MO is nanopowder.

Since combining MO with the AC having nanoporous (CNP) may shorten the diffusion length and improving the conductivity [6-7]. Since the PSC depends on the applied voltage, therefore AC/MO supercapacitor may produce a higher capacitance and provide a bigger potential window when non-aqueous electrolyte used. The simplest way to prepare a composite of AC/MO is by mixing them. The information on optimizing such a composition still requires further investigation. Study of supercapacitors based on the composite of AC and nano MO materials have been reported [8-10]. Ref. [9] reviewed the potential of nano MnO_2 and activated carbon. Ref. [10] said that using composite nano MnO_2 and AC having mesoporous increased the surface area, improved the conductance, and increased the capacitance of supercapacitor. It also reported that using that AC and nanoparticles MnO_2 as low as 5% in weight increased the capacitance almost twice more compared to the AC supercapacitor. However, the mechanism of increasing the specific capacitance still requires more explanation.

Chmiola et al. [11] indicated that the appearance of the microporous in of carbon having high surface area contributing to such increment. In this investigation, we pursue to clarify this mechanism is happening in AC/MO supercapacitor. Further, since the use of composite electrodes consisting of reduced graphene oxide (RGO) and CNP with first activation using 100 ^oC may improve the conductance and increase the active surface area [12]. High capacitance of supercapacitor about 330 Fg^{-1} [12] was achieved by coating MnO_2 on top of the graphene oxide layer. Up to now, fabricating AC based supercapacitor have still drawn the interest of many authors [13-15]. Some effort was spent to modify nanostructure both the AC and the MO [13-15]. A high capacitance value, 464 Fg^{-1} at ten mV/s, was obtained using AC fiber having nanosize pores and nanosphere MnO_2 [13]. A better supercapacitor AC and various nanostructure MnO_2 particles produced capacitance 248.3-824.8 Fg^{-1} at five mV/s [14]. Both were in thousands cycle stability [13-14]. It was reported that coating carbon fabric with AC fibers and MnO_2 nanoparticles was only reaching the capacitance value of 169 Fg^{-1}. Ref. [12] inspired us to study the effect of the addition of RGO on top of the AC/MO electrodes and to heat it to 120 ^oC in the effort of modifying the nanosurface of AC/MO/RGO.

2. Materials and Method

2.1 Materials

The activated carbon, derived from the coconut shell, was prepared using a method taken from Ref.[13]. In short, we did the process in two steps. The first step was carbonization. We did it using the oven at 900 ^oC. The next step was activation in which the carbon was pulverized and soaked in the alkaline solution for 36 hours, before heating under tubular furnace at 850 ^oC in the oxygen atmosphere. The nano-TMO were purchased from Merck and used without any treatment. The average size of CuO, TiO_2, MnO_2 were about 50 nm. We also used other material such as PVDF sheet (EMCO), carbon black (Sigma Aldrich), and DMF (Sigma Aldrich) without any modification.

2.2 Methods of preparing the supercapacitors

We developed the electrodes by mixing the AC (200 mesh) with 5% weight of black carbon in dimethylacetamide solution. We form an own mixture of 5%, 10%, 15%, and 20% weight nano metal oxide (CuO, TiO_2, MnO_2) with the solution. We stirred each solution to form it as a slurry using 200 rpm within 6 hours at 100

^{o}C. We build the electrodes using that mixture by pasting it on the aluminum foil, as the current collector, using a doctor blade apparatus. The composite film was then dried within 30 minutes in the desiccator at 100 ^{o}C. We constructed a symmetric supercapacitor using polyvinylidene difluoride as the membrane with 3 M KOH as the electrolyte in a coin shell. The thickness of the composite film was approximately 100 μm. The weight was about 2.5 mg, and the size was of a half inch. Since our experiment indicating that electrodes of made of AC and 5% (CuO, TiO_2, MnO_2) producing maximum capacitance, we built up the AC/MO/RGO by adding the solution of 2% RGO in water on top of AC/MO surface. The RGO solution was put in ultrasonication for 30 minutes. Then AC/MO/RGO composite was heated again at 100 ^{o}C assuming the layers of RGO formed on top of AC/MO surface.

2.3 Methods of characterization

We checked the porosity of the composite using BET method (Nova 4200e) using N_2 gas. We obtained the micro image (JSM 6390A) and made the mapping the element using SEM (Hitachi SU 3500). We examined the nanoparticles image using TEM (FEI Techni G2 20). We tested the crystalline of the materials and the composite using XRD (Shimadzu R6000) using Cu as the cathode with a scan rate of 0.5^{o} s^{-1}. The performance of the supercapacitor was done using two-probe cyclic voltammetry (CV) (Wontech WBCS 3000). To measure the electrochemical property, we set the electrochemical impedance spectroscopy (EIS) operating at the frequency from 0.5 mHz up to 4 MHz. The capacitance was calculated by integrating the CV curves to find the charge, *Q*, divided by the window voltage, *V*, and the mass of the electrodes *m*. It was expressed in Fg^{-1}. To compare the capacitance of AC, AC/MO, and AC/MO/RGO supercapacitors, we set CV in scan speed of 10 mVs^{-1}. In the galvanostatic test, we use a current of 2 Ag^{-1}. Acquiring the above data, we can calculate the energy and power density in unit Wh/kg and W/kg respectively, and study the performance of the supercapacitors.

3. Result and Discussion

Fig. 1. showed the TEM image of TiO_2, CuO, and MnO_2 respectively to confirm average size of metal oxide particles still about 50 nm.

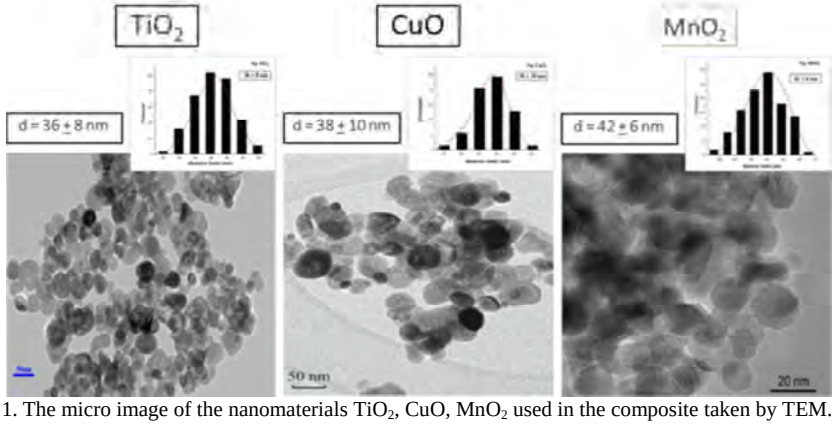

Fig 1. The micro image of the nanomaterials TiO_2, CuO, MnO_2 used in the composite taken by TEM.

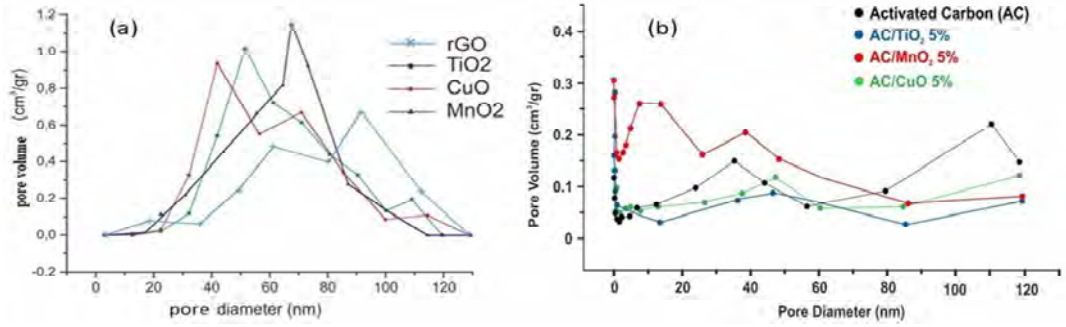

Fig 2. The porosity distribution of the electrodes of (a) AC/MO/RGO (MO = TiO_2, CuO, MnO_2), as well as (b) AC/MO.

The pores distribution of the RGO, TiO_2, CuO, and MnO_2, as well as AC/MO, was shown in Fig. 2(a) and 2(b) respectively. Fig. 2(a). indicated that the maximum pore volume of particles of RGO, TiO_2, CuO, and MnO_2 was in the range of 0.6 cm^3g^{-1} to 1.1 cm^3g^{-1}. Amongst these particles, RGO had more pores greater than 80 nm compared to TiO_2, CuO, and MnO_2. The pore size showed the RGO was in the form of bulk since in the form layer the range of pore were less than 20 nm [13]. By heating the RGO solution and putting on top of AC/MO, we expected that the pores in the region greater than 70 nm become less dominant. On the other side, Fig. 2(b) presented the pores distribution of AC and AC/TiO_2, AC/CuO, and AC/MnO_2. Fig. 2(a), told us that the mixing of AC and MO suppressed the pores in the area greater than 80 nm belongs to AC. The volume of the pores in AC/MO was smaller compared to ones in Fig. 2(a), as well as the size of the pores that of in the AC. This situation indicated that the pores in AC/MO would be nearer to the interface of the electrode and the electrolyte. The pores of AC/MO would make it easier to develop PSC mechanism when in contact with an electrolyte.

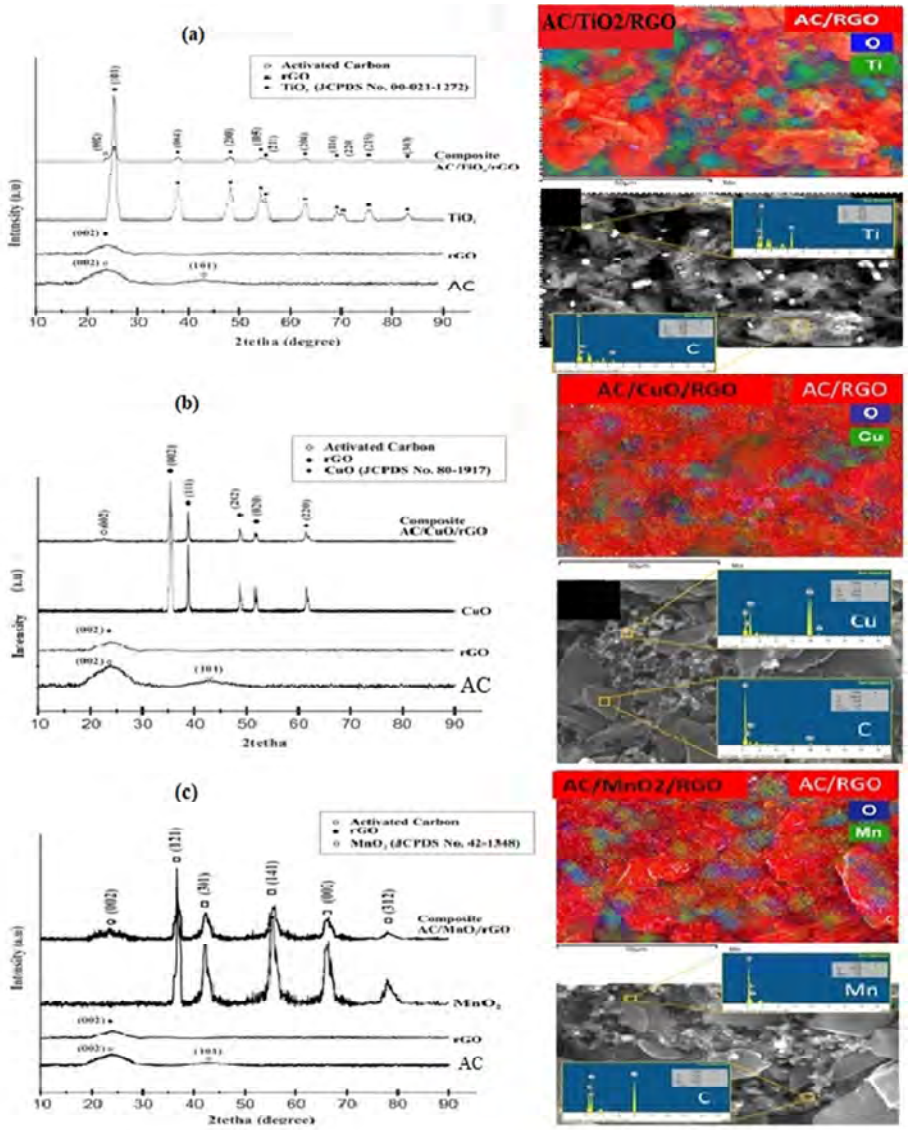

Fig. 3. XRD and SEM EDX of elements and the composite of (a) the AC, RGO, CuO, AC/CuO/RGO; (b) AC, RGO,TiO_2, AC/TiO_2/RGO; and (c) AC, RGO, MnO_2, AC/MnO_2/RGO.

The XRD spectra of the components and the composite consisting C, MO TiO_2, CuO, and MnO_2 = 5%), and RGO (2%) as well as the mapping of the elements in the electrodes, were shown in Fig.3. The picture in Fig. 3(a), (b), (c) presented that the peak belongs to [101] plane did not appear in the RGO. Fig. 3(a), (b), and (c) also showed that there was no significant difference between the XRD spectra of the components and the composite. In other words, the electrodes were in the state of a composite. Fig. 3(a) also showed the mapping of the elements of carbon, Ti and O on the electrodes using EDS. The mapping of Ti, Cu, Mn, and O in Fig. 3(a), 3(b) and 3(c) showed that the elements Ti, Cu, and Mn were distributed randomly on the surface. The existence of MO on the surface of the electrodes was essential to explain the possibility of PSC mechanism. The O element was in a more dominant part compared to those elements, while C was the primary component. We concerned only with the nanoparticles of MO in the concentration of 5% since our previous investigation indicated that this concentration producing the maximum capacitance as presented in Ref. [10].

To see the roles of RGO in the AC/MO/RGO electrodes, we measured the CV of the supercapacitors at the scan rate of $10mVs^{-1}$ and its impedance. We tested the impedance of AC/MO and AC/MO/RGO using EIS in the frequency range of 0.5 mHz to 4MHz. Fig. 4(a) showed the CV curves of the two-probe test. In Fig. 4(a), we noticed the existence of weak EDLC with a robust PSC mechanism at AC/MO/RGO. In contrast, in Fig. 4(e)-4(g), we found the robust EDLC mechanism in synergic with PSC at AC/MO curves. This difference was due to variations of the surface area in both composites. Because the capacitance of AC/MO/RGO was smaller than that of AC/MO, therefore, the charge time was also faster.

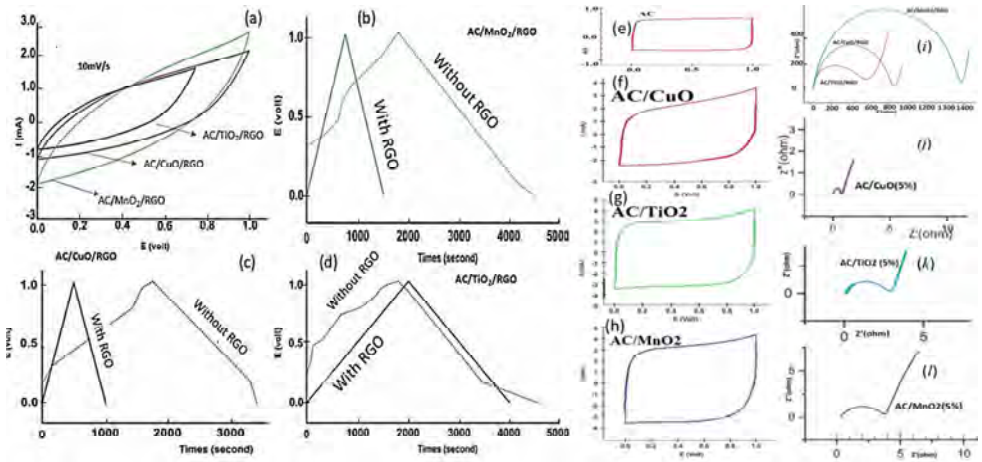

Fig. 4. The CV curves of (a) the supercapacitor AC/MO/RGO,charge-discharge curves of AC/MO/RGO and AC/MO at 2 Ag^{-1}: (b); (c); (d); and the CV curves of the (c) AC/CuO; (g) AC/TiO_2; and (g) AC/MnO_2 followed by the impedance of the supercapacitors (h)AC/MO/RGO; (i)AC/CuO; (j) AC/TiO_2; and AC/MnO_2.

Table 1. Performance of supercapacitor based on activated carbon (AC), metal oxide (MO), and reduced graphene oxide (RGO). The specific capacitance and energy was calculated at scan rate 10 mVs^{-1}. The power was calculated from discharge time using current $2Ag^{-1}$.

Electrode	Surface area (m^2/g)	Cs (F/g)	Energi (Wh/kg)	Discharge time (s)	Power (W/kg)
AC	1570	100	27.8	450	61.7
AC/CuO (5%)	1613	280	77.8	2700	28.8
AC/TiO_2 (5%)	1560	290	80.6	2200	36.6
AC/MO_2 (5%)	1701	372	103.3	1900	54.4
AC/CuO (5%) RGO (2%)	870	50	13.9	500	27.8
AC/TiO_2 (5%) RGO (2%)	678	34	9.4	2000	4.7
AC/MO_2 (5%) RGO (2%)	1120	80	22.2	1000	22.2

The impedance of AC/MO/RGO, AC, and AC/MO, and was shown in Fig. 4(i)-4(l), respectively. The series resistance, $R_{s,}$ was the intercept of Z' at the lowest frequency, while ion transfer resistance, R_{ct}, was the intercept of Z' at the highest frequency. In AC/MO/RGO, the R_{ct}=700 Ω belonged to AC/TiO_2/RGO was the smallest. In AC/TiO_2, the R_{ct} = 3.2 Ω. In short R_{ct} in AC/MO/RGO was about hundreds times bigger than that of AC/MO. These

values told that the electrochemical process in AC/MO was much superior to the one in AC/MO/RGO. This feature was also another effect due to the bulk RGO. The value was also shown in Table 1.

Finally, the addition RGO could only boost the charging times but not the capacitance and energy density. However, the capacitance of AC/MnO_2 obtained in this article was comparable to the ones obtained by other authors in Ref. [12-13,15] but it was still lower compared to some of the results in Ref. [14].

4. Conclusion

It has been fabricated and studied the symmetric supercapacitors of AC/MO/RGO using a simple casting process of RGO on top of AC/MO surface and heating the surface. The method used in making the supercapacitor was not able to facilitate the RGO in the layers form. Instead, it was in the state of bulk. This bulk RGO caused the surface area to be smaller, the diameter of the pores become bigger than in AC/MO, and made the synergy between EDLC and PCS mechanism weaker. Although its energy density was significantly lower compared to that of AC/MO, the AC/MO/RGO had a shorter charging rate.

Acknowledgement

The research was made possible due to the grant from Hibah Penelitian BOPTN FMIPA Universitas Gadjah Mada in the year 2018 and due to the supporting from Laboratorium Fisika LIPI, Serpong, Indonesia.

References

[1] J. Gamby, P.L Taberna, P. Simon, J.F Fauvarque, M.Chesneau, J. Power Sorce. 101 (2001) 109-116.
[2] D. Seng Su and R. Schlögl, Chem.Sus. Chem. 3 (2010) 136-168.
[3] L. Demarconnay, E. Raymundo-Piñero, F. Béguin, J. Electrochem. Comm. 12 (2010) 1275-1278
[4] A. Jain, V. Aravindan, S. Jayaraman, P.S. Kumar, R. Balasubramanian, S. Ramakrishna, S. Madhavi, M.P. Srinivasan, Sci. Rep. 3 (2013) 3002.
[5] S. Faraji, F. Nasir Aini, Ren. Sust. En. Rev. 42 (2015) 823-834.
[6] Singh, A. Chandra, Sci. Rep. 5 (2016) 15551.
[7] M. Zhi, C. Xiang, J. Li, M. Li, N. Wu, Nanoscale. 5 (2013) 72-88.
[8] Y. Wang, Jin Guo, T. Wang, J. Shao, D. Wang, Y.W. Yang, Nanomaterials (Basel). 5 (2015) 1667–1689.
[9] C.M. Yulien, A. Mauger, Nanomaterials. 7 (2017) 396.
[10] M. Doloksaribu, Harsojo, K. Triyana, B. P. Handoko, Internat. Jour. of App. Eng. Res. 12 (2017) 8625-8631.
[11] J. Chmiola, G. Yushin, Y.Gogotsi, C. Portet, P. Simon, P.L. Taberna, Science. 313 (2006) 760.
[12] L.L. Zhang, X. Zhao,M.D. Stoller, Y. Zhu, H. Ji, S. Murali,Y. Wu, S. Perales, B. Clevenger, R.S. Ruoff, J. NanoLett. 12 (2012) 1806−1812.
[13] T. Hu, X. Chu, F. Gao, Y. Dong, W. Sun, L. Bai, Mat. Sci. Semicon. Proc. 34 (2015) 146–153.
[14] H. Shen, Y. Zhang, X. Song,Y. Liu, H. Wang, H. Duan, X. Kong, J Alloys Compd. 770 (2019) 926-933.
[15] A.J. Paleo, P. Staiti, A. Brigandì, F.N. Ferreira, A.M. Rocha, F. Lufrano, J. En. Store. Mat. (2018) 204-215.